International Journal of Bifurcation and Chaos, Vol. 8, No. 6 (1998) 1183–1197

NONLINEAR RESONANCE IN BASIN PORTRAITS OF TWO COUPLED SWINGS UNDER PERIODIC FORCING

YOSHISUKE UEDA and YOSHINORI UEDA
Department of Electrical Engineering, Kyoto University, Kyoto 606-8501, Japan

H. BRUCE STEWART
Department of Applied Science, Brookhaven National Laboratory, Upton, New York 11973, USA

RALPH H. ABRAHAM
Mathematics Department, University of California, Santa Cruz, CA 95064, USA

Received November 14, 1997; Revised December 5, 1997

A model of a simple electric power supply network involving two generators connected by a transmission network to a bus is studied by numerical simulation. In this model, the bus is supposed to maintain a voltage of fixed amplitude, but with a small periodic fluctuation in the phase angle. In such a case, traditional analysis using direct methods is not applicable. The frequency of the periodic fluctuation is varied over a range of values near a nonlinear resonance of the two-generator network. When the bus fluctuation frequency is away from resonance, the system has several attractors; one is a small-amplitude periodic oscillation corresponding to synchronized, quasi-normal operation (slightly swinging), while others are large amplitude periodic oscillations which, if realized, would correspond to one or both generators operating in a desynchronized steady state.

When the bus fluctuation frequency approaches resonance, a new periodic attractor with large amplitude oscillations appears. Although it does correspond to a synchronized steady state, this attractor has a disastrously large amplitude of oscillation, and represents an unacceptable condition for the network. Basin portraits show that this resonant attractor erodes large, complicated regions of the basin of the safe operating condition. Under conditions of small periodic fluctuation in bus voltage, this basin erosion would not be detected by traditional analysis using direct methods. Further understanding of such complicated basin structures will be essential to correctly predict the stability of electric power supply systems.

1. Introduction

The stability of electric power systems is a well-established subject with a long history of research [Anderson & Fouad, 1994]. Stability problems have become more complex as interconnections become more extensive and systems operated closer to capacity. There is growing recognition that phase space geometric concepts and dynamical bifurcation theory can provide some of the tools necessary to understand power system stability.

The question of transient stability has been studied primarily through differential equation models based on the swing equation or driven pendulum. While realistic problems may involve coupled systems of hundreds or even thousands of equations, it is sometimes helpful to consider small prototype systems where fundamental concepts can be more clearly apprehended.

Here we propose to extend our previous research in this area [Ueda *et al.*, 1991, 1992] by again

considering a model system consisting of two generators connected to a bus by a simple transmission network. In contrast to the previous work, here, we consider that the bus does not maintain a constant voltage, but rather the bus voltage has constant amplitude, with small periodic fluctuations in the phase angle which act as a forcing term, unaffected by the two generators [Yorino *et al.*, 1985a, 1985b, 1988; Tamura, 1992].

We again focus attention on the basins of attraction of this model, maintaining as before that in many practical situations the first true and proper concern of the engineer should be the extent in phase space of the basin of attraction of the safe operating condition. For example, when a system operates in a very noisy environment, such as a ship in heavy seas, the engineer must be prepared to consider the ultimate fate of a system trajectory over time begun from a wide range of initial conditions. Likewise in a power system, when a fault occurs, the system may find itself in any of a wide range of states immediately after the fault is detected and cleared. The question is whether such a state evolves under the dynamics of the post-fault system to a stable and safe operating condition; in other words, whether the immediate post-fault state is in the basin of attraction of the safe operating condition.

The particular phenomenon we consider here is the possibility that a small swing in one part of a large power supply network may excite a nonlinear resonance and hence produce a disproportionately large swing in another part of the system. We represent the small exciting swing as a bus whose phase angle has a small sinusoidal forcing term; the excited subsystem is the two generators and their associated transmission lines.

2. System Definition with Parameters and Forcing

In this paper we consider the following system of ordinary differential equations for two coupled swings under periodic forcing:

$$\begin{aligned}
\frac{d\delta_1}{d\tau} &= \omega_1 \\
\frac{d\omega_1}{d\tau} &= p_1 - b_{12}\sin(\delta_1 - \delta_2) \\
&\quad - b_{1B}\sin(\delta_1 - \delta_B) - D_1\omega_1 \\
\frac{d\delta_2}{d\tau} &= \omega_2 \\
\frac{d\omega_2}{d\tau} &= a\{p_2 - b_{21}\sin(\delta_2 - \delta_1) \\
&\quad - b_{2B}\sin(\delta_2 - \delta_B) - D_2\omega_2\}\,. \qquad (1)
\end{aligned}$$

Here the independent variable (normalized time) is denoted by τ. The dependent variables δ_1, δ_2 are the angular displacements of generators 1 and 2, respectively, and ω_1, ω_2 are the angular velocities of generators 1 and 2.

The equations involve several parameters. The parameter a is the inertia ratio of the two generators (which are assumed to have the same rated capacity). The parameters p_1 and p_2 represent the mechanical input powers to the generators, and the parameters b_{12}, b_{21}, b_{1B}, and b_{2B} depend on the electrical properties of the network. The coefficients D_1 and D_2 are damping constants; δ_B stands for the phase of the bus voltage.

The derivation of this system of ordinary differential equations from an electric network is given in the Appendix A.

Table 1 shows the values chosen for the system parameters in our present studies.

The goal of this study is to investigate the influence of bus fluctuations on the basins of attraction of the system (1), and our aim is simply to illustrate basic phenomena which will be of fundamental importance in better understanding the stability of electric power systems.

We considered two different types of fluctuations. In one type, the voltage magnitude at the bus is considered constant, while the phase angle δ_B at the bus undergoes a sinusoidal oscillation described by

$$\delta_B = \theta_B \sin \Omega t \qquad (2)$$

so that the system becomes

$$\begin{aligned}
\frac{d\delta_1}{d\tau} &= \omega_1 \\
\frac{d\omega_1}{d\tau} &= p_1 - b_{12}\sin(\delta_1 - \delta_2) \\
&\quad - b_{1B}\sin(\delta_1 - \theta_B \sin \Omega t) - D_1\omega_1 \\
\frac{d\delta_2}{d\tau} &= \omega_2 \\
\frac{d\omega_2}{d\tau} &= a\{p_2 - b_{21}\sin(\delta_2 - \delta_1) \\
&\quad - b_{2B}\sin(\delta_2 - \theta_B \sin \Omega t) - D_2\omega_2\}\,.
\end{aligned} \qquad (3)$$

Table 1. Numerical values chosen for the parameters in the fluctuating bus model Eqs. (1).

a	p_1	p_2	b_{12}	b_{21}	b_{1B}	b_{2B}	D_1	D_2
0.8	0.2	0.3	0.4	0.4	1.4	1.4	0.005	0.005

In a second type of fluctuation, the phase angle is assumed fixed at $\delta_B = 0$ while the magnitude of the bus voltage fluctuates. Thus b_{1B}, b_{2B} would be replaced by

$$b_{1B}(1+\varepsilon \sin \Omega t), \quad b_{2B}(1+\varepsilon \sin \Omega t). \tag{4}$$

Basin portraits obtained using both types of fluctuation share many qualitative features. Since the phase fluctuation in a real power system is usually more significant than voltage fluctuation, we present in this paper only the results of the phase fluctuation equations (3).

3. Unperturbed Case

We first consider the unperturbed case [Ueda *et al.*, 1991, 1992] in which there is no fluctuation in either amplitude or phase at the bus. We then have the autonomous system

$$\begin{aligned}
\frac{d\delta_1}{d\tau} &= \omega_1 \\
\frac{d\omega_1}{d\tau} &= p_1 - b_{12}\sin(\delta_1-\delta_2) - b_{1B}\sin\delta_1 - D_1\omega_1 \\
\frac{d\delta_2}{d\tau} &= \omega_2 \\
\frac{d\omega_2}{d\tau} &= a\{p_2 - b_{21}\sin(\delta_2-\delta_1) - b_{2B}\sin\delta_2 - D_2\omega_2\}.
\end{aligned} \tag{5}$$

For our chosen parameter values, this system has four distinct equilibrium point solutions. The stability of each equilibrium is determined by the eigenvalues of the matrix

$$\begin{bmatrix}
0 & 1 & 0 & 0 \\
-b_{12}\cos(\delta_1-\delta_2) - b_{1B}\cos\delta_1 & -D_1 & b_{12}\cos(\delta_1-\delta_2) & 0 \\
0 & 0 & 0 & 1 \\
ab_{21}\cos(\delta_2-\delta_1) & 0 & -ab_{21}\cos(\delta_2-\delta_1) - ab_{2B}\cos\delta_2 & -aD_2
\end{bmatrix}.$$

Table 2 shows the numerical values of the equilibrium point coordinates and their eigenvalues.

Equilibrium point 0 is the stable operating condition. It has two eigenfrequencies or resonant frequencies: $\Omega_1 = 1.095$ corresponds to a mode in which the two generators oscillate in phase, while the higher frequency $\Omega_2 = 1.415$ corresponds to a mode with the two generators oscillating out of phase. The remaining equilibrium points are unstable.

Traditionally, the stability of the system (5) has been analyzed with the aid of the following first integral or energy function for the unperturbed system without damping:

$$\begin{aligned}
V(\delta_1, \omega_1, \delta_2, \omega_2) \equiv{}& \frac{1}{2}\omega_1^2 + \frac{1}{2a}\omega_2^2 - p_1\delta_1 - p_2\delta_2 \\
&- b_{12}\cos(\delta_1-\delta_2) - b_{1B}\cos\delta_1 \\
&- b_{2B}\cos\delta_2 .
\end{aligned} \tag{6}$$

This function has the property that along any solution of the autonomous system

$$\frac{dV}{d\tau} = -D_1\omega_1^2 - D_2\omega_2^2 \le 0. \tag{7}$$

Traditionally the stability analysis of the system (5) uses direct methods based on the following argument: Select the equilibrium point having the second lowest value of V (in this case, point 2), and let this value of V be called V_c; then the hypersurface $V = V_c$ represents a sufficient condition for stability.

We now examine the basins of attraction of the unperturbed system by systematic integrations from a large number on initial conditions. A complete basin portrait of the system would require the full four-dimensional phase space; fortunately, much information can be gained from a few two-dimensional slices through the phase space. The following four slices will be used for all our basin portraits: In the plane (δ_1, δ_2); in the plane (δ_1, ω_1); in the plane (δ_2, ω_2); and in the plane (ω_1, ω_2). In each case the section passes through the stable equilibrium point 0.

Figure 1 shows the results of integrations in these four sections. In each case, initial conditions on a grid of 101 × 101 points were integrated. Figure 1 is composed of 101 × 101 small squares,

Table 2. Location and stability of the equilibrium points of the unperturbed system Eqs. (5), with the parameter values in Table 1.

	Equilibrium Point 0	Equilibrium Point 1	Equilibrium Point 2	Equilibrium Point 3
δ_1	0.156616	3.100081	0.245942	3.047650
ω_1	0	0	0	0
δ_2	0.202549	0.321134	3.027673	2.875112
ω_2	0	0	0	0
Eigenvalues	$-0.002 + j1.095$	$-0.002 + j1.015$	$-0.002 + j0.898$	-1.122
	$-0.002 - j1.095$	$-0.002 - j1.015$	$-0.002 - j0.898$	-0.717
	$-0.002 + j1.415$	-1.206	-1.350	0.713
	$-0.002 - j1.415$	1.206	1.350	1.117

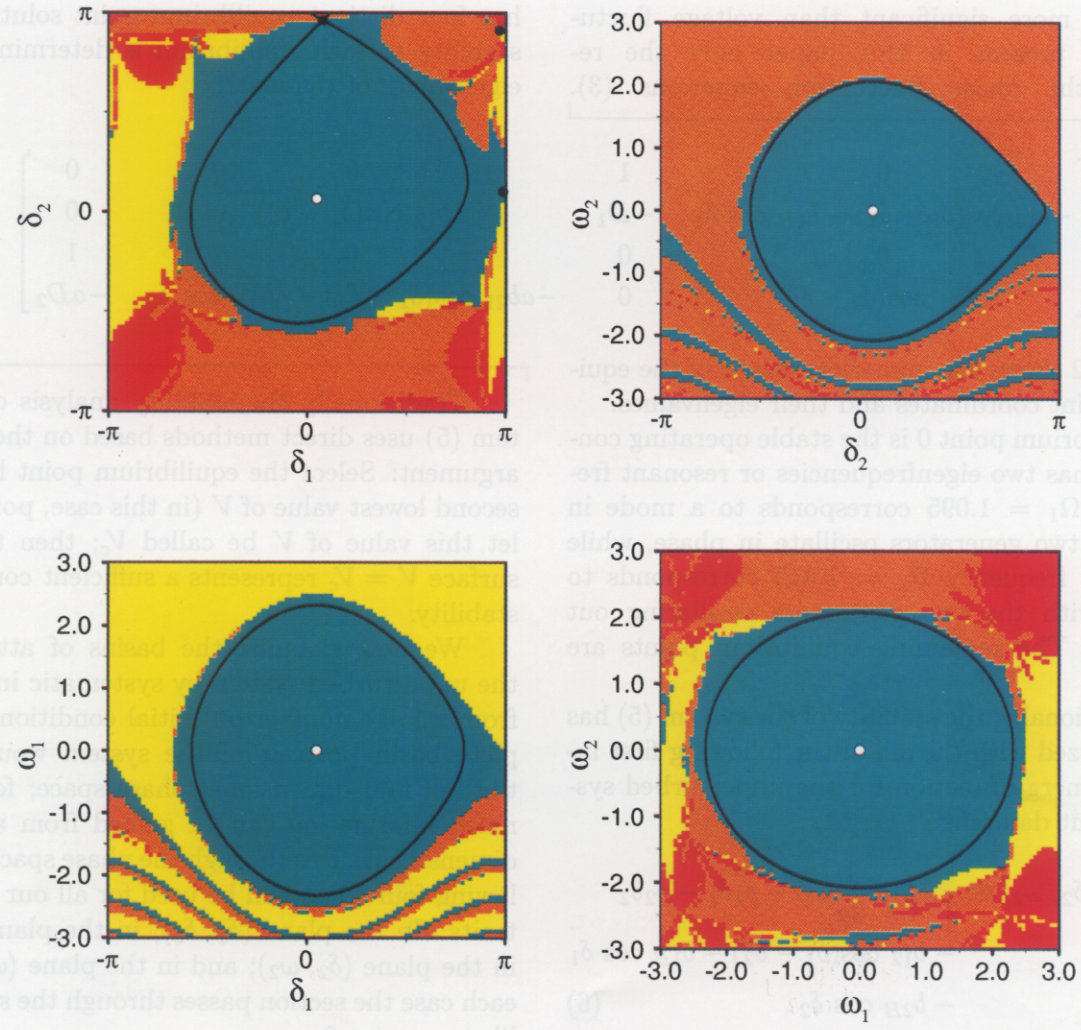

Fig. 1. Sectional basin portraits of the unperturbed system Eqs. (5), showing the stable equilibrium point (white dot), unstable equilibrium points (black dots), and intersections with the hypersurface $V = V_c$. The basins are colored light blue for the desirable steady operating condition, and red, orange and yellow for basins of undesirable desynchronized attractors.

Table 2. Location and stability of the equilibrium points of the unperturbed system Eqs. (5), with the parameter values in Table 1.

	Equilibrium Point 0	Equilibrium Point 1	Equilibrium Point 2	Equilibrium Point 3
δ_1	0.156616	3.100081	0.245942	3.047650
ω_1	0	0	0	0
δ_2	0.202549	0.321134	3.027673	2.875112
ω_2	0	0	0	0
Eigenvalues	−0.002 + j1.095	−0.002 + j1.015	−0.002 + j0.898	−1.122
	−0.002 − j1.095	−0.002 − j1.015	−0.002 − j0.898	−0.717
	−0.002 + j1.415	−1.206	−1.350	0.713
	−0.002 − j1.415	1.206	1.350	1.117

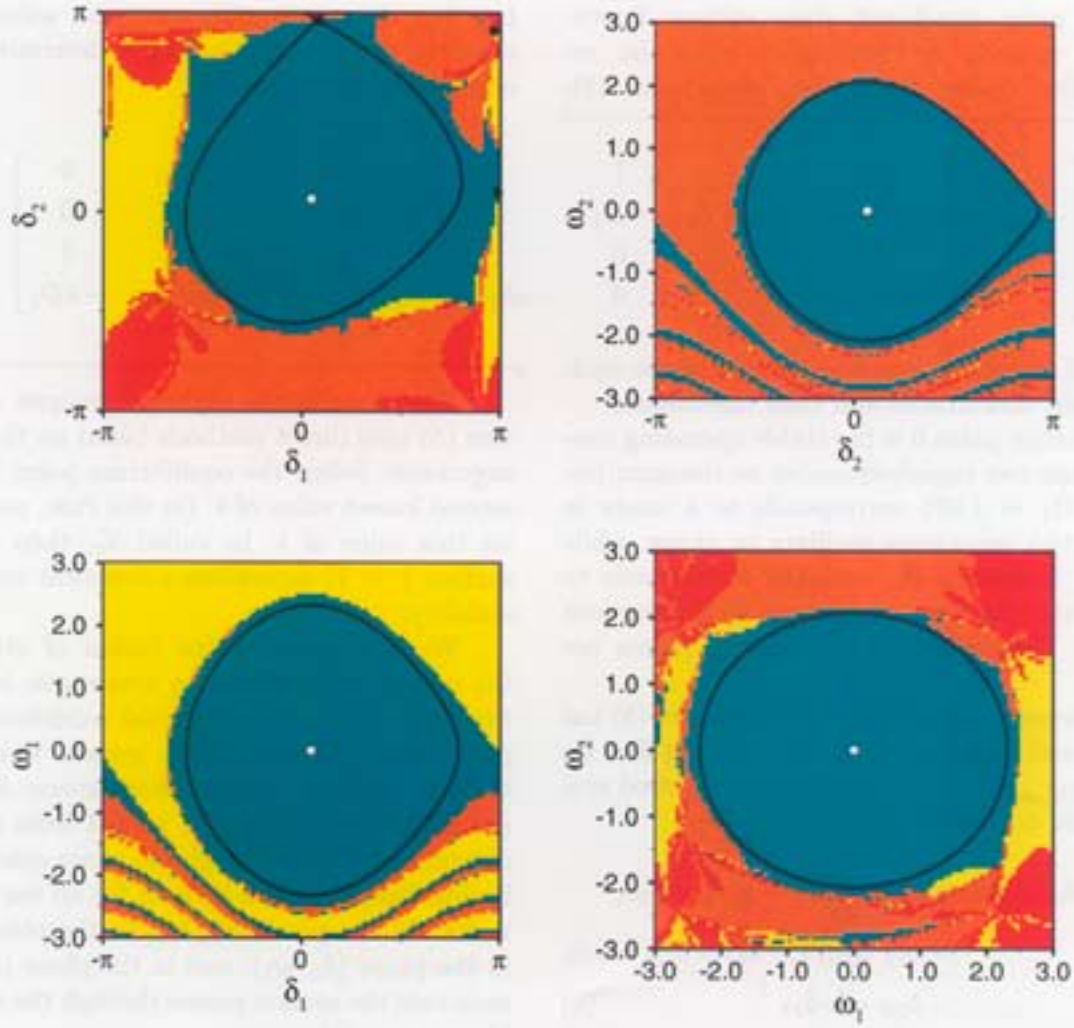

Fig. 1. Sectional basin portraits of the unperturbed system Eqs. (5), showing the stable equilibrium point (white dot), unstable equilibrium points (black dots), and intersections with the hypersurface $V = V_c$. The basins are colored light blue for the desirable steady operating condition, and red, orange and yellow for basins of undesirable desynchronized attractors.

each colored according to the particular attractor ultimately reached by the corresponding initial condition. At these parameter values, the system has four attractors. One attractor is equilibrium point 0, representing the stable operating condition; its basin is colored *light blue.* A second attractor is a stable periodic orbit, in which generator 1 steps out and sustains oscillations desynchronized from the bus; its basin is colored *yellow.* A third attractor is similar except that generator 2 is desynchronized; its basin is *orange.* The fourth attractor represents a sustained oscillation in which both generators are desynchronized from the bus; its basin is *red.* Of course none of the three periodic attractors would be realized in an actual power system: The desynchronized oscillations would destroy the generator(s). But the basins themselves are of paramount importance: if the state of a power system immediately after a fault were within the yellow, orange, or red basins, intervention would be required to avoid a potentially destructive transient.

Also shown in Fig. 1 are the curves where each two-dimensional slice of phase space intersects the hypersurface $V = V_c$. From these sectional views, it appears that the hypersurface $V = V_c$ encloses a convex region lying entirely in the light blue basin of the safe operating condition, as guaranteed by the theory for the unperturbed system.

4. Fluctuating Bus and Resonance

We now consider the system (3) in which the bus is supposed to undergo a small sinusoidal swing in phase angle. It is well known that sinusoidal forcing may excite a nonlinear resonance in a system operating within a smooth potential well, if for example the potential well departs from quadratic shape due to a smooth potential barrier over which the system may escape from the well. Such resonance arises from the nonlinear softening of the restoring force as the system is forced up the potential barrier, and occurs for forcing frequencies somewhat less than the natural frequency of small unforced oscillation near the bottom of the well [Thompson, 1989; Soliman & Thompson, 1989; Stewart *et al.*, 1995].

The swing equation has just such a nonquadratic potential well; crossing the potential barrier is equivalent to stepping out. It should therefore be no great surprise that the system (3) exhibits nonlinear resonance associated with stepping out and desynchronization. With the small amount of dissipation typical of power systems, these resonances may be very strong, so that a jump to resonance would be just as dangerous and potentially destructive as desynchronization.

To analyze the resonant response of the system (3), numerical solutions were approximated by Fourier sine series expansions for the displacements δ_1 and δ_2:

$$\begin{aligned}\delta_1(\tau) &= \delta_{10} + \delta_{11}\sin(\Omega\tau - \phi_{11}) \\ &\quad + \delta_{12}\sin(2\Omega\tau - \phi_{12}) + \cdots \\ \delta_2(\tau) &= \delta_{20} + \delta_{21}\sin(\Omega\tau - \phi_{21}) \\ &\quad + \delta_{22}\sin(2\Omega\tau - \phi_{22}) + \cdots .\end{aligned} \tag{8}$$

The Fourier coefficients δ_{ij}, $i = 1, 2$, $j = 0, 1, 2$, were computed for many solutions at different values of Ω. Figure 2 shows results plotted over a range of Ω values spanning the linear resonant frequencies in Table 2, and with $\theta_B = 0.01$.

The resonance at the lower frequency, corresponding to an in-phase oscillation, is very strong. The first harmonic components δ_{i1} show dramatically a typical nonlinear resonant response, bent toward lower frequencies as expected for a softening of the restoring force. There is an extended range of frequencies at which the resonant solution coexists with the nonresonant solution. (The intervening unstable solution branch is not shown.)

This and similar scans of approximate resonant response guide our choice of conditions for which bus fluctuations are of special concern, where basin portraits should be examined. Here we present two sequences of basin portraits. The first sequence, shown in Fig. 3, was taken at $\theta_B = 0.01$ and a succession of frequencies Ω spanning the stronger resonance in Fig. 2. The basin colors are as in Fig. 1: The basin of the stable operating condition is again colored *light blue.* Also, we now use an additional color, *dark blue*, to indicate the basin of attraction of the resonant solution. Again we emphasize that although this solution corresponds to synchronized operation, with neither generator stepping out, nevertheless the resonant solution may represent an intolerable condition for the system.

Progressing in frequency Ω through the basin portraits in Fig. 3, and comparing with Fig. 2, we see that at frequencies such as $\Omega = 0.84$ and $\Omega = 0.88$, where the resonant response has the largest amplitude, the corresponding erosion of the light blue basin by the dark blue resonant basin is slight. However, for higher frequencies such as $\Omega = 1.0$ and $\Omega = 1.04$, the resonant response

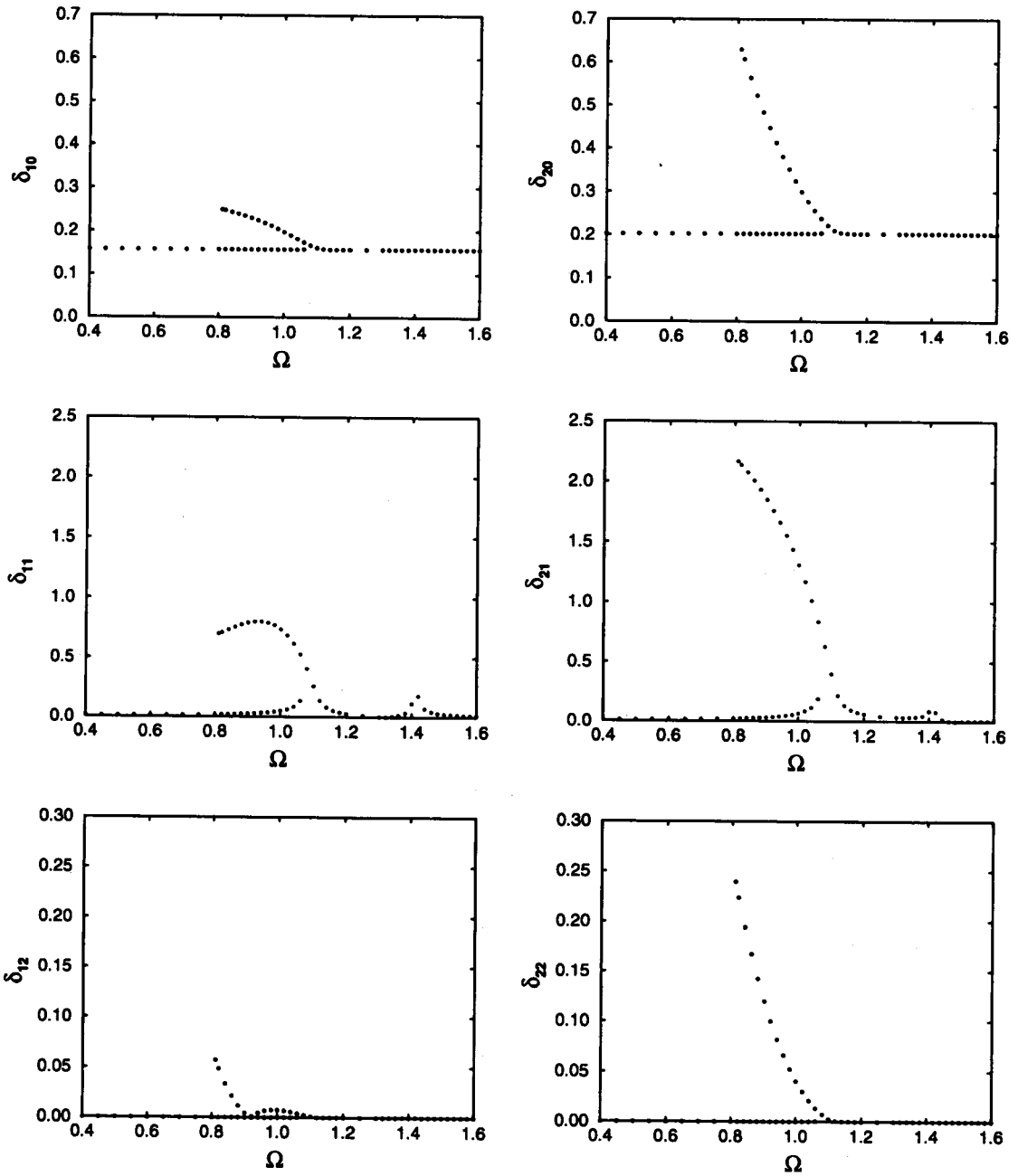

Fig. 2. Low-order Fourier coefficients of nonlinear resonant solutions of the system Eqs. (3) with fluctuating bus angle, for $\theta_B = 0.01$ and a range of frequencies Ω.

amplitude is still large, while the light blue basin has been severely eroded. Comparing with Fig. 1, we see that the hypersurface $V = V_c$ is no longer a conservative or even a sufficient condition for the system to reach a desirable steady state, because of erosion by the dark blue resonant basin.

At the highest frequency shown, namely $\Omega = 1.08$, the dark blue region has completely eroded the light blue basin. Note however that here the resonant response amplitude is not nearly so large; indeed, there are no longer two co-existing synchronized attractors. So the dark blue region may now represent the return to an acceptable steady operating condition. The significance of the dark blue region in each basin portrait should be evaluated with reference to the response amplitudes indicated in Fig. 2. Taking this into account, it is still clear that the energy function method may fail to detect serious dangers which are clearly indicated by sample basin portraits.

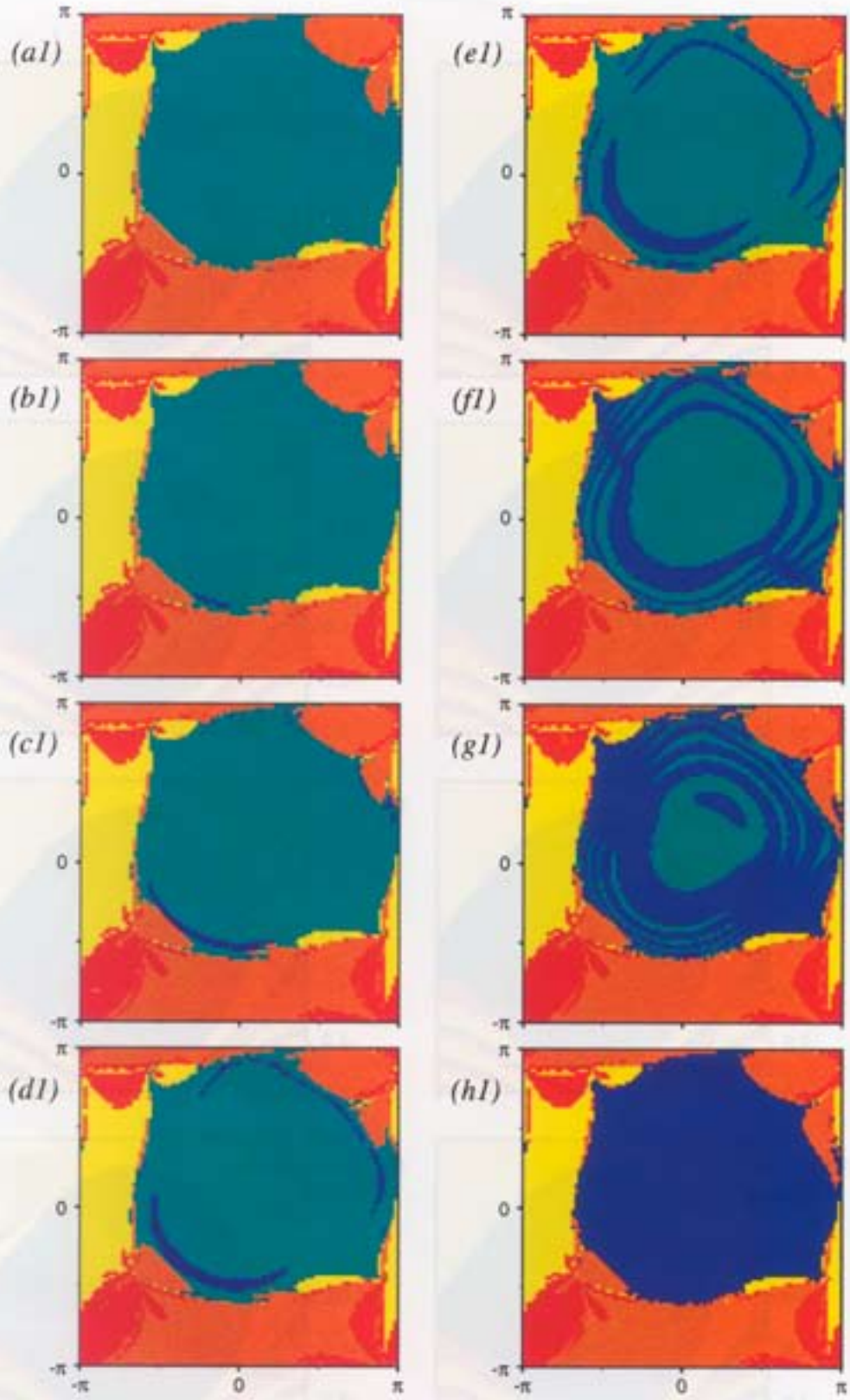

Fig. 3. Sequence of sectional basin portraits of the system Eqs. (3) with fluctuating bus angle, for $\theta_B = 0.01$ and eight different frequencies Ω near the strongest resonance. Cases (a) $\Omega = 0.80$, (b) $\Omega = 0.84$, (c) $\Omega = 0.88$, (d) $\Omega = 0.92$, (e) $\Omega = 0.96$, (f) $\Omega = 1.00$, (g) $\Omega = 1.04$, and (h) $\Omega = 1.08$; sequences (1) in the plane (δ_1, δ_2), (2) in the plane (δ_1, ω_1), (3) in the plane (δ_2, ω_2) and (4) in the plane (ω_1, ω_2). Basin colors for the desynchronized attractors are as in Fig. 1; the color dark blue is added for the basin of the resonant synchronized attractor, which erodes the light blue basin of the desirable operating condition.

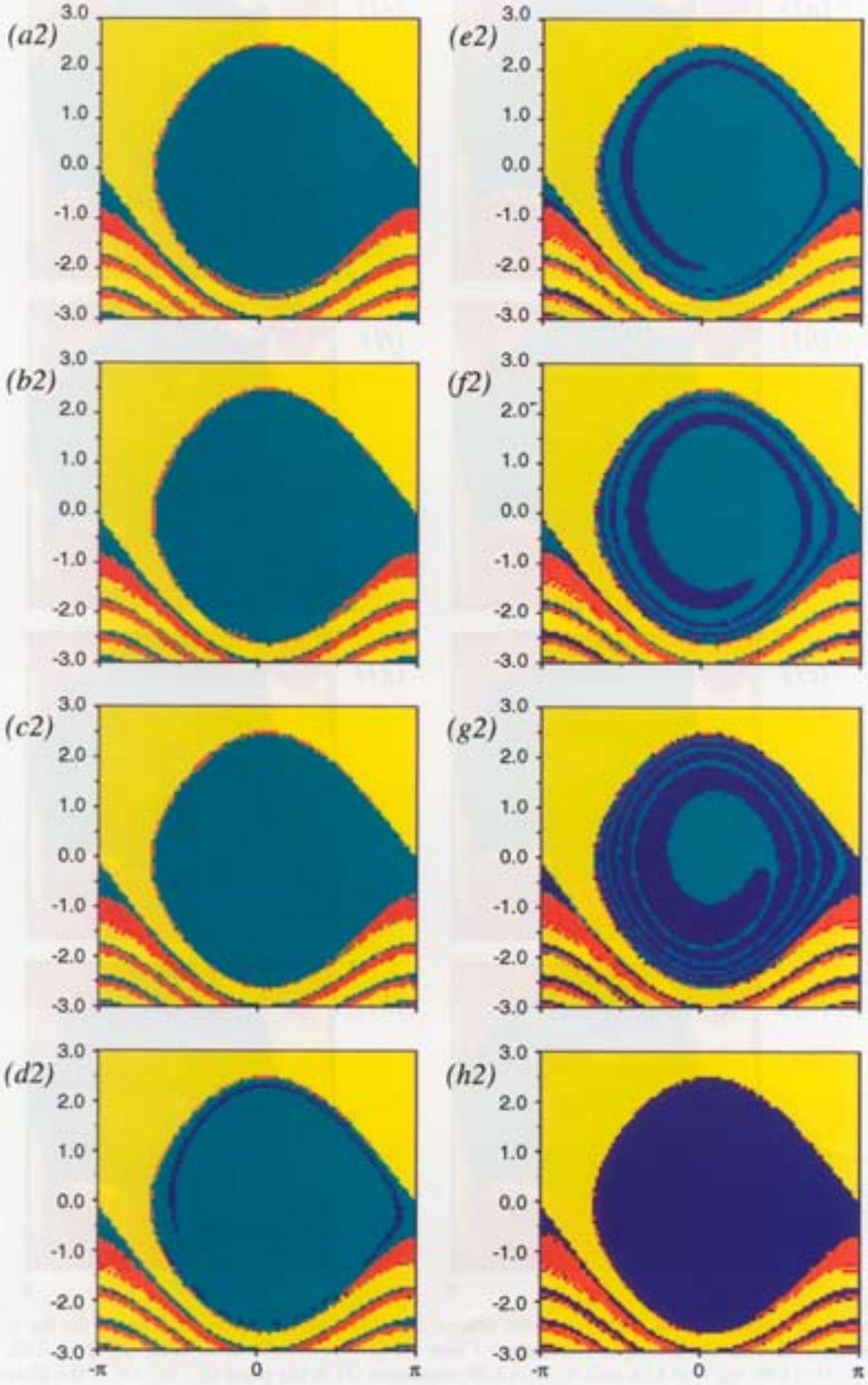

Fig. 3. (*Continued*)

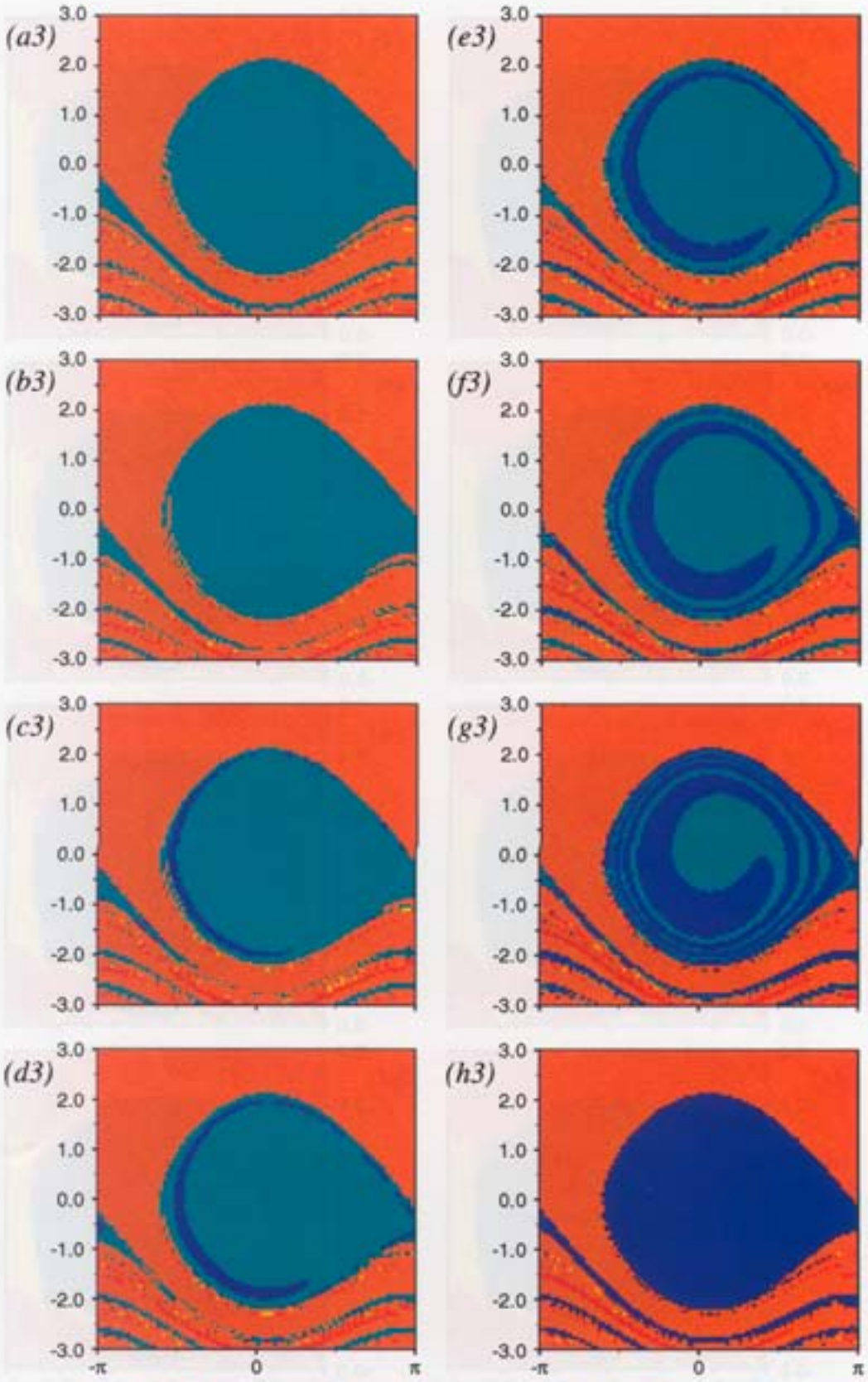

Fig. 3. (*Continued*)

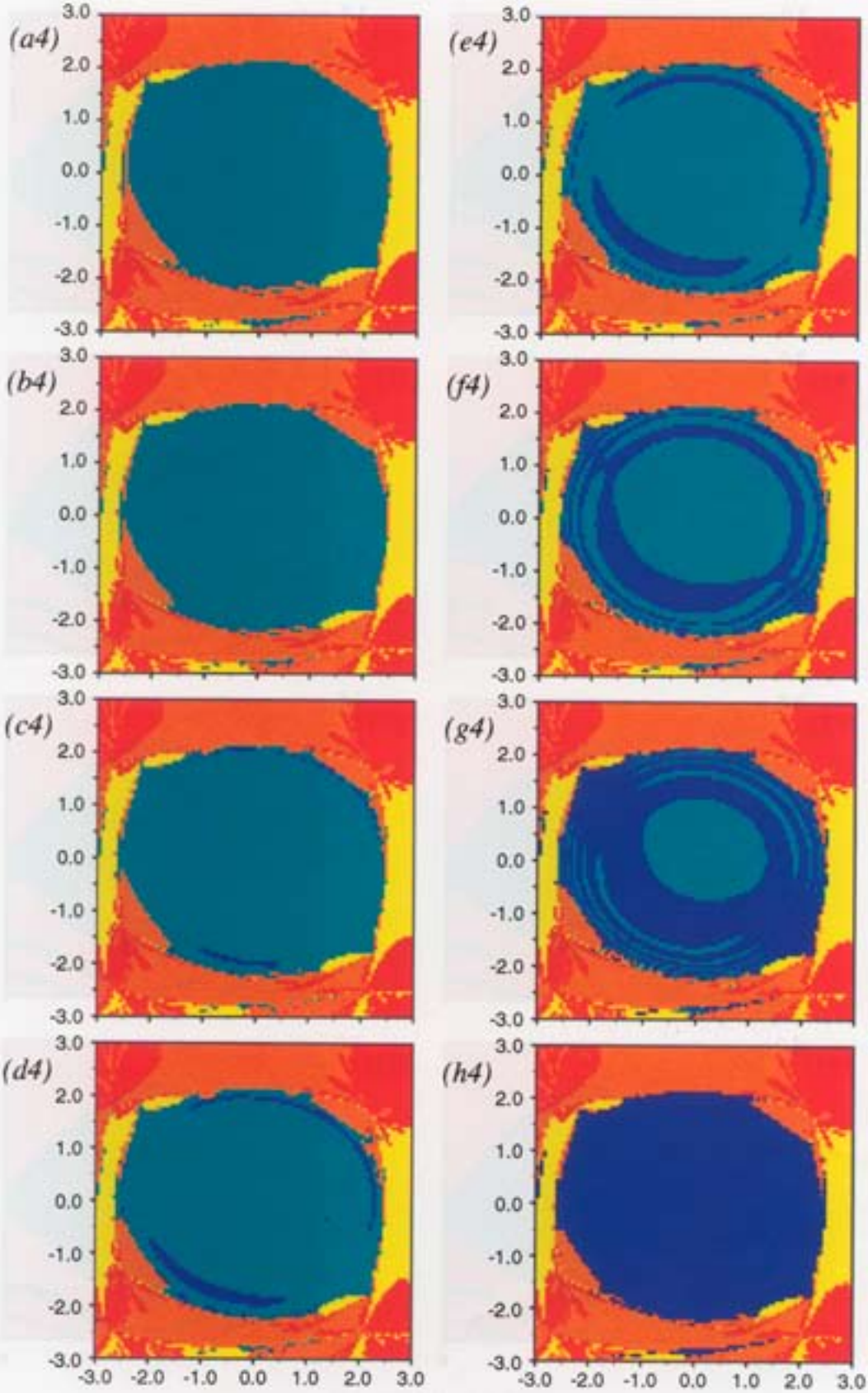

Fig. 3. (*Continued*)

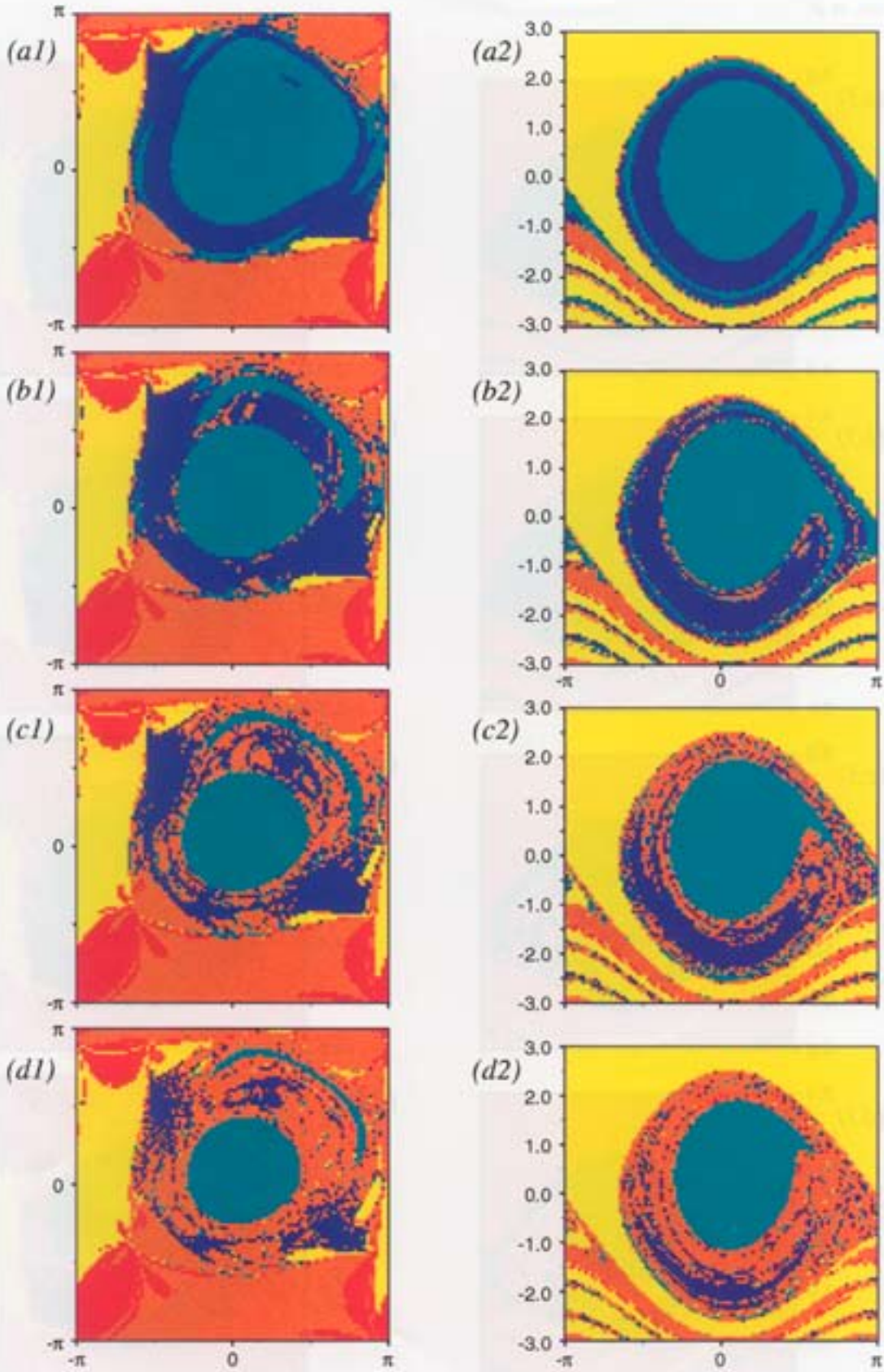

Fig. 4. Sequence of sectional basin portraits of the system Eqs. (3) with fluctuating bus angle, for $\Omega = 0.95$ and four different values of the amplitude θ_B of bus angle fluctuation. Cases (a) $\theta_B = 0.02$, (b) $\theta_B = 0.03$, (c) $\theta_B = 0.04$, (d) $\theta_B = 0.05$; sequences (1) in the plane (δ_1, δ_2), (2) in the plane (δ_1, ω_1), (3) in the plane (δ_2, ω_2), and (4) in the plane (ω_1, ω_2). Basin colors as in Fig. 3, showing further erosion of the basin of the desirable operating condition.

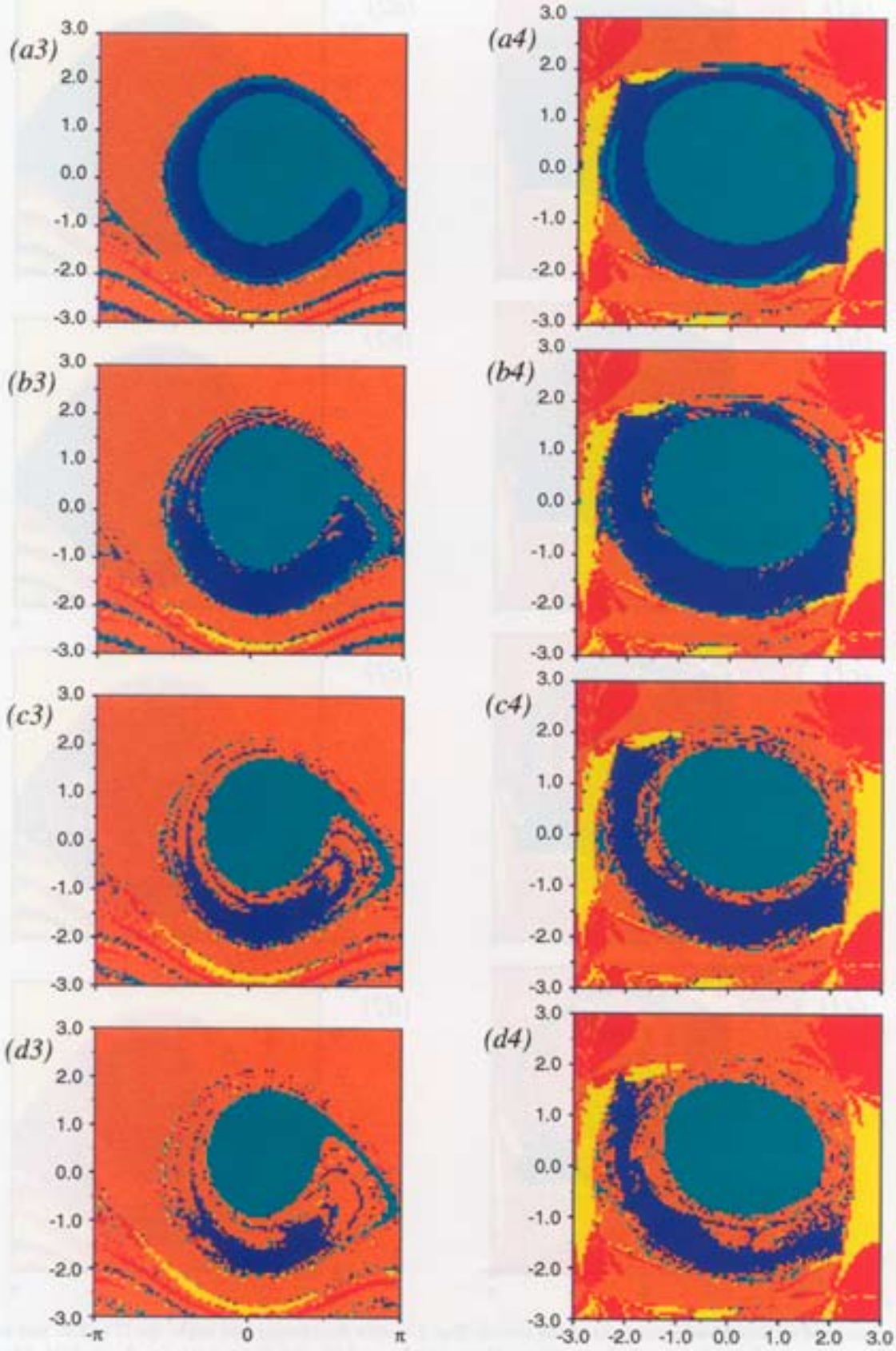

Fig. 4. (*Continued*)

A second series of basin portraits is shown in Fig. 4. Here the frequency Ω of bus fluctuation is 0.95 in every case, and the magnitude of bus angle fluctuation increases to $\theta_B = 0.05$ in steps of 0.01. Further approximate solutions similar to those in Fig. 2 showed that the resonant response at $\theta_B = 0.05$ is similar to that at $\theta_B = 0.01$. At $\theta_B = 0.05$ the out-of-phase resonance is somewhat stronger; the frequency range and the peak response amplitude of the in-phase resonance are about the same as at $\theta_B = 0.01$, while the nonresonant response amplitude has increased. The frequency $\Omega = 0.95$ used for Fig. 4 still corresponds to an unacceptable condition reached from the dark blue basin, which further erodes the light blue basin.

Another disturbing aspect of the basin portraits in Fig. 4 is that the light blue basin is eroded not only by the dark blue resonant basin, but also by the orange basin of a desynchronized attractor as well. Further exploratory simulations of the system (3) by numerical integration confirmed that a jump to resonance provoked by slowly varying Ω may be *indeterminate* [Thompson & Soliman, 1991; Stewart & Ueda, 1991], with the outcome attractor (resonant or desynchronized) depending very sensitively on the details of how the jump is provoked, such as the rate of scanning Ω, or a small amount of noise.

Furthermore, we note that the yellow basin and the red basin do not noticeably participate in the erosion of the light blue basin. In other words, the basin erosion threatens to cause step out of generator 2, but the threat of generator 1 stepping out is negligible. (This is due to our choice of parameters, which is not symmetric: The power output p_2 of generator 2 is larger than the output p_1 of generator 1, and also the ratio of inertias a is not one.) Thus the basin portraits in Fig. 4, sequence 2 in the (δ_1, ω_1) plane show the safe basin surrounded by yellow basin (generator 1 steps out), but eroded by the orange basin (generator 2 steps out). Although resonance and basin erosion can occur in a periodically forced one-machine system, the basin erosion pattern in Fig. 4 can only be observed in a system with more than one machine.

References

Anderson, P. M. & Fouad, A. A. [1994] *Power System Control and Stability* (New York, IEEE Press).

Soliman, M. S. & Thompson, J. M. T. [1989] "Integrity measures quantifying the erosion of smooth and fractal basins of attraction," *J. Sound Vibration* **135**, 453–475.

Stewart, H. B., Thompson, J. M. T., Ueda, Y. & Lansbury, A. N. [1995] "Optimal escape from potential wells — patterns of regular and chaotic bifurcation," *Physica* **D85**, 259–295.

Stewart, H. B. & Ueda, Y. [1991] "Catastrophes with indeterminate outcome," *Proc. Roy. Soc. London* **A432**, 113–123.

Tamura, Y. [1993] "Possibility of parametric resonance in power systems," *IEEJ* **112**, 657–663.

Thompson, J. M. T. [1989] "Chaotic phenomena triggering the escape from a potential well," *Proc. Roy. Soc. London* **A421**, 195–225.

Thompson, J. M. T. & Soliman, M. S. [1991] "Indeterminate jumps to resonance from a tangled saddle-node bifurcation," *Proc. Roy. Soc. London* **A432**, 101–111.

Ueda, Y., Noriyasu, M. & Stewart, H. B. [1991] "Analysis of basic sets on basin boundaries using straddle orbit method on a two-degree-of-freedom swing equation," (in Japanese) IEICE (Japan) Report NLP91-43.

Ueda, Y., Enomoto, T. & Stewart, H. B. [1992] "Chaotic transients and fractal structures governing coupled swing dynamics," in *Applied Chaos*, eds. Kim, J. H. & Stringer, J. (New York, John Wiley), pp. 207–218.

Yorino, N., Mori, H. & Tamura, Y. [1985a] "On the relationship between power system stability and parametric resonance," *IEEJ* **B105**, 15–22.

Yorino, N., Nagashima, Y., Kubota, T., Mori, H. & Tamura, Y. [1985b] "On parametric resonance in power systems," *IEEJ* **B105**, 805–812.

Yorino, N., Tamura, Y. & Sasaki, H. [1988] "On autoparametric resonance in power systems and method of its analysis," *IEEJ* **B108**, 321–328.

Appendix A
Derivation of the System of Equations (1)

With the notation of Fig. A, the equations for the network are written as

$$\dot{E}_1 - \dot{E}_B = jx_1\dot{I}_1 + jx(\dot{I}_1 + \dot{I}_2)$$
$$\dot{E}_2 - \dot{E}_B = jx_2\dot{I}_2 + jx(\dot{I}_1 + \dot{I}_2)\,.$$

From the above we get

$$\dot{I}_1 = \frac{1}{\Delta}\{-j(x + x_2)\dot{E}_1 + jx\dot{E}_2 + jx_2\dot{E}_B\}$$
$$\dot{I}_2 = \frac{1}{\Delta}\{-j(x + x_1)\dot{E}_2 + jx\dot{E}_1 + jx_1\dot{E}_B\}$$

where

$$\Delta = (x + x_1)(x + x_2) - x^2\,.$$

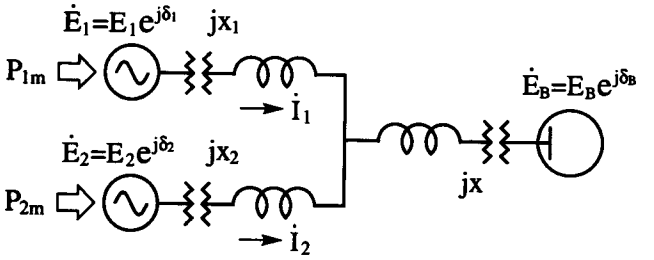

Fig. A. Schematic diagram of a power supply network with two generators connected by transmission lines to a slightly fluctuating bus.

The outputs of the generators are

$$P_{1e} = \Re(\dot{E}_1\bar{I}) = \frac{1}{\Delta}\{xE_1E_2\sin(\delta_1-\delta_2) + x_2E_1E_B\sin(\delta_1-\delta_B)\}$$

$$P_{2e} = \Re(\dot{E}_2\bar{I}) = \frac{1}{\Delta}\{xE_1E_2\sin(\delta_2-\delta_1) + x_1E_2E_B\sin(\delta_2-\delta_B)\}.$$

The equation of motion (without dissipation) of the rotor of generator 1 is

$$I_{1R}\frac{d^2\theta_1}{dt^2} = T_{1m} - T_{1e}$$

where

I_{1R} = rotor moment of inertia
θ_1 = rotor angular displacement
$= \omega_B t + \delta_1$
ω_B = system angular frequency
T_{1m} = mechanical input torque
T_{1e} = electromagnetic torque

and similarly for generator 2. By definition

$$P_{1m} = \dot{\theta}_1 T_{1m}$$
$$P_{1e} = \dot{\theta}_1 T_{1e}$$

and

$$\dot{\theta}_1 = \omega_B + \dot{\delta}_1.$$

Therefore we obtain

$$I_{1R}\frac{d^2\theta_1}{dt^2} = I_{1R}\frac{d^2\delta_1}{dt^2} \simeq \frac{1}{\omega_B}(P_{1m}-P_{1e})$$

and similarly for generator 2

$$I_{2R}\frac{d^2\theta_2}{dt^2} = I_{2R}\frac{d^2\delta_2}{dt^2} \simeq \frac{1}{\omega_B}(P_{2m}-P_{2e}).$$

Now we may substitute the expressions for the output of the generators to obtain

$$\frac{\omega_B I_{1R}}{P_B}\frac{d^2\delta_1}{dt^2} = \frac{P_{1m}}{P_B} - \frac{xE_1E_2}{\Delta P_B}\sin(\delta_1-\delta_2) - \frac{x_2E_1E_B}{\Delta P_B}\sin(\delta_1-\delta_B)$$

$$\frac{\omega_B I_{2R}}{P_B}\frac{d^2\delta_2}{dt^2} = \frac{P_{2m}}{P_B} - \frac{xE_1E_2}{\Delta P_B}\sin(\delta_2-\delta_1) - \frac{x_1E_2E_B}{\Delta P_B}\sin(\delta_2-\delta_B)$$

where

P_B = volt-ampere base quantity.

Rewriting this in terms of normalized quantities gives

$$\frac{\omega_B I_{1R}}{P_B}\frac{d^2\delta_1}{dt^2} = p_1 - b_{12}\sin(\delta_1-\delta_2) - b_{1B}\sin(\delta_1-\delta_B)$$

where

$$p_1 = \frac{P_{1m}}{P_B}$$

$$b_{12} = \frac{xE_1E_2}{\Delta P_B}$$

$$b_{1B} = \frac{x_2E_1E_B}{\Delta P_B}$$

and

$$\frac{\omega_B I_{2R}}{P_B}\frac{d^2\delta_2}{dt^2} = p_2 - b_{21}\sin(\delta_2-\delta_1) - b_{2B}\sin(\delta_2-\delta_B)$$

where

$$p_2 = \frac{P_{2m}}{P_B}$$

$$b_{21} = \frac{xE_1E_2}{\Delta P_B}$$

$$b_{2B} = \frac{x_1E_2E_B}{\Delta P_B}.$$

The normalization of time appropriate for generator 1 is

$$\tau = \sqrt{\frac{P_B}{\omega_B I_{1R}}}\cdot t$$

which leads to the ordinary differential equations:

$$\frac{d^2\delta_1}{d\tau^2} = p_1 - b_{12}\sin(\delta_1 - \delta_2) - b_{1B}\sin(\delta_1 - \delta_B)$$

$$\frac{d^2\delta_2}{d\tau^2} = a\{p_2 - b_{21}\sin(\delta_2 - \delta_1) - b_{2B}\sin(\delta_2 - \delta_B)\}.$$

Here

$$a = \frac{I_{1R}}{I_{2R}} = \frac{H_1}{H_2}$$

is the ratio of inertias, alternatively expressed as a ratio of per-unit inertia constants H_1, H_2 defined by

$$\frac{2H_1}{\omega_B} = \frac{\omega_B I_{1R}}{P_B}$$

$$\frac{2H_2}{\omega_B} = \frac{\omega_B I_{2R}}{P_B}.$$

Note that in this paper the two generators are assumed to have the same rated capacity.

Finally we include a damping term for each generator proportional to its angular velocity. In keeping with the simple character of the model, we use a constant damping coefficient. The final working form of the differential equations is then

$$\frac{d^2\delta_1}{d\tau^2} = p_1 - b_{12}\sin(\delta_1 - \delta_2) - b_{1B}\sin(\delta_1 - \delta_B) - D_1\frac{d\delta_1}{d\tau}$$

$$\frac{d^2\delta_2}{d\tau^2} = a\left\{p_2 - b_{21}\sin(\delta_2 - \delta_1) - b_{2B}\sin(\delta_2 - \delta_B) - D_2\frac{d\delta_2}{d\tau}\right\}.$$

Appendix B
Comments on the Numerical Values of the Parameters

In Appendix A we presented the derivation of the swing equations (1), including expressions for the parameters b_{12}, b_{21}, b_{1B}, and b_{2B} in terms of the network reactances x, x_1, and x_2. It is also possible to reverse this procedure, and calculate the reactances x, x_1, and x_2 from the values of the parameters in Table 1 together with values of E_1, E_2, E_B, and P_B. The reader who is interested in real power systems will be able to choose reasonable values for E_1, E_2, E_B, and P_B, and may then use the following relations to get an idea of the system we had in mind when we chose the parameter values in Table 1:

$$x_1 = \frac{b_{2B}E_1^2E_2E_B}{P_B\{(b_{12}E_B + b_{2B}E_1)(b_{12}E_B + b_{1B}E_2) - b_{12}^2E_B^2\}}$$

$$x_2 = \frac{b_{1B}E_1E_2^2E_B}{P_B\{(b_{12}E_B + b_{2B}E_1)(b_{12}E_B + b_{1B}E_2) - b_{12}^2E_B^2\}}$$

$$x = \frac{b_{12}E_1E_2E_B^2}{P_B\{(b_{12}E_B + b_{2B}E_1)(b_{12}E_B + b_{1B}E_2) - b_{12}^2E_B^2\}}.$$

We note that the reactance values so obtained include not only that of the transmission line, but also the leakage reactance of the power station transformer, and the reactance of the generator in transient states, for appropriate values of E_1 and E_2.